

Large Language Models for Single-Step and Multi-Step Flight Trajectory Prediction

Kaiwei Luo
School of Computer Science
Sichuan University
Chengdu, China
kevin_rowe_it_sc@stu.scu.edu.cn

Jiliu Zhou*
School of Computer Science
Sichuan University
Chengdu, China
zhoujl@cuit.edu.cn

Abstract—Flight trajectory prediction is a critical time series task in aviation. While deep learning methods have shown significant promise, the application of large language models (LLMs) to this domain remains underexplored. This study pioneers the use of LLMs for flight trajectory prediction by reframing it as a language modeling problem. Specifically, We extract features representing the aircraft’s position and status from ADS-B flight data to construct a prompt-based dataset, where trajectory waypoints are converted into language tokens. The dataset is then employed to fine-tune LLMs, enabling them to learn complex spatiotemporal patterns for accurate predictions. Comprehensive experiments demonstrate that LLMs achieve notable performance improvements in both single-step and multi-step predictions compared to traditional methods, with LLaMA-3.1 model achieving the highest overall accuracy. However, the high inference latency of LLMs poses a challenge for real-time applications, underscoring the need for further research in this promising direction.

Index Terms—large language models, flight trajectory prediction, deep learning, single-step and multi-step prediction

I. INTRODUCTION

Air Traffic Management (ATM) faces significant challenges arising from the increasing density of flight activities. The rapid growth of the global economy has significantly boosted the demand for air transportation across various industries, causing higher airspace complexity [1]. To tackle these challenges, substantial global efforts have been made to develop more efficient air traffic systems. For instance, the United States has introduced the Next Generation Air Transportation System (NextGEN) [2] to modernize the national airspace, while Europe has launched the Single European Sky ATM Research (SESAR) [3] program to optimize air traffic management across member states. Both initiatives rely on Trajectory-Based Operations (TBO) for ATM automation [4]. As an essential component of TBO, flight trajectory prediction systems ensure accurate and timely support in many ATM scenarios, such as conflict detection [5], flight delay forecasting [6], and air traffic flow management [7].

Flight trajectory prediction is often viewed as a multivariate time series problem. Depending on the prediction horizon, time series tasks are categorized into single-step and multi-step prediction, as shown in Fig. 1. In single-step prediction,

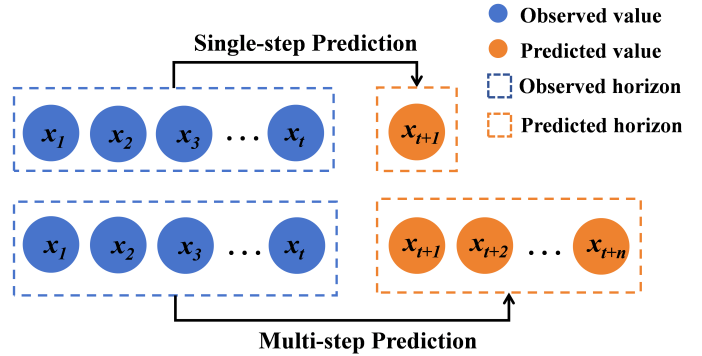


Fig. 1. Overview of single-step and multi-step prediction in time series tasks.

the model predicts only the next immediate value, while in multi-step prediction, it forecasts multiple future values in one go. The primary goal of trajectory prediction is to forecast the future status parameters of aircraft, such as longitude, latitude, altitude, and velocity, based on the observed historical data [8]. Trajectory prediction can be further divided into short-term and long-term categories based on the time scale [9]. Short-term prediction emphasizes real-time responsiveness in dynamic environments, providing high-precision position estimates over short periods. In contrast, long-term prediction offers a broader perspective for strategic planning by incorporating external factors such as flight intentions and environmental data, but suffers from growing uncertainty and computational overhead. Therefore, this work focuses on short-term prediction in both single-step and multi-step scenarios, relying exclusively on historical status parameters.

Great efforts have been made in flight trajectory prediction, evolving from physics-based [10], [11], [12] to data-driven approaches [13], [14], [15]. Physics-based methods typically model the interactions between the aircraft and environment using aerodynamics and kinematic equations. However, these models are too idealized to make accurate predictions in dynamic real-time air traffic systems [16]. With the rise of deep learning, new avenues have been opened for prediction tasks. Deep learning models effectively capture complex air traffic dynamics from historical flight data, making them the most prevailing approach for this task. In recent years, large language models (LLMs) have advanced rapidly and

*Corresponding author.

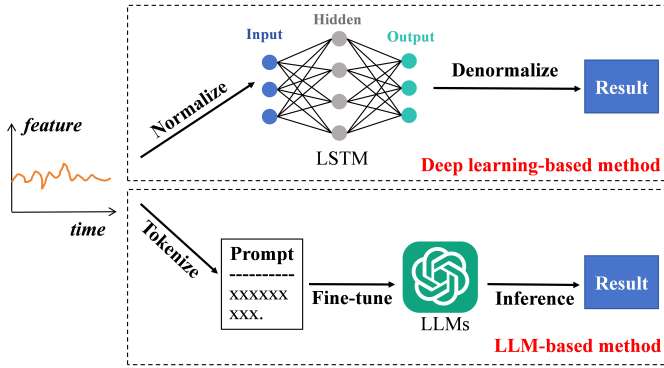


Fig. 2. Comparison of deep learning-based (e.g. LSTM) and LLM-based methods in time series tasks.

been successfully applied to various areas, including computer vision [17], [18], speech recognition [19], and autonomous driving [20], demonstrating exceptional potential in solving complex challenges. The comparison of deep learning-based methods and LLM-based methods is detailed in Fig. 2.

As shown in Fig. 2, neural network (e.g., LSTM [21]), along with its variants, is widely used in deep learning-based methods, where data is normalized to unify feature scales. However, normalization introduces drawbacks as well, such as diluted data distribution, reduced data discrimination, and unexpected output when the input is out of range. LLM-based methods significantly reduce the reliance on explicit normalization by adopting a structured workflow comprising tokenization, prompt construction, fine-tuning, and inference.

While LLMs have demonstrated remarkable success across multiple domains, their potential in flight trajectory prediction remains insufficiently explored. To this end, this study investigates the capabilities of LLMs in trajectory prediction. Specifically, we extract relevant features representing flight status from Automatic Dependent Surveillance-Broadcast (ADS-B) [22] data and incorporate them into domain-specific prompts. We then apply Parameter-Efficient Fine-Tuning (PEFT) to various open-source LLMs, enabling them to learn underlying patterns from historical flight data. Finally, we predict future trajectories using the fine-tuned LLMs. Our contributions can be summarized as follows:

- We propose FTP-LLM (Large Language Models for Flight Trajectory Prediction), a novel framework that reformulate the prediction task as a language modeling problem. To the best of our knowledge, this is the first study to apply LLMs to flight trajectory prediction.
- We construct datasets based on ADS-B flight data, and design aviation domain-specific prompt templates tailored for single-step and multi-step trajectory prediction.
- We conduct extensive experiments to evaluate eight state-of-the-art LLMs, showcasing their strong performance and notable few-shot generalization capabilities in flight trajectory prediction.

The remainder of this paper is organized as follows: Section II provides a review of related work on flight trajectory prediction; Section III details the proposed methodology and

model architecture; Section IV presents experimental results, analysis, and visualizations; and Section V concludes with a discussion of future research directions.

II. RELATED WORK

A. Flight Trajectory Prediction

Existing approaches in flight trajectory prediction are classified into state estimation, kinetic, and data-driven methods.

1) *State Estimation Methods*: State estimation methods regard trajectory prediction as a mathematical state transition problem, focusing on dynamic state parameters like position, velocity, and acceleration. Kalman Filter (KF) and Hidden Markov Model (HMM) are two widely used state estimation techniques: KF is efficient for linear systems, while HMM excels in modeling discrete state transitions. Jeung et al. [23] employed HMMs to overcome the limitations of traditional space-partitioning methods in trajectory pattern mining. Wang et al. [10] enhanced 4D trajectory prediction with a real-time noise-adaptive Kalman Filter. Rezaie et al. [11] introduced a conditionally Markov sequence to model airliner trajectories using waypoint data. Despite their effectiveness, state estimation models struggle with nonlinear dynamics in the real-time systems due to simplified equations.

2) *Kinetic Methods*: Kinetic methods predict flight trajectories by modeling the relationships between forces and aircraft motion using differential equations. These models incorporate the aircraft's current state, meteorological conditions, and flight intent [24]. Schuster et al. [12] developed a 4D gate-to-gate model leveraging aircraft state and intent to enhance accuracy and air traffic management. Sun et al. [25] inferred aircraft takeoff mass using a kinetic model and recursive runway motion data estimation. Besada et al. [26] introduced intent-based formal languages and a trajectory processing engine for automated, hierarchical trajectory computation. In summary, kinetic methods rely on idealized assumptions, thus overlooking real-world constraints and human factors. Additionally, their reliance on extensive external data undoubtedly increases the computational intensity.

3) *Data-Driven Methods*: Data-driven methods, which are primarily classified into machine learning and deep learning models, have attracted significant attention for their ability to directly learn patterns from data. Tastambekov et al. [27] introduced an algorithm employing local linear functional regression, integrating wavelet decomposition for data preprocessing and regression, to predict 4D short- to mid-term aircraft trajectories. De Leege et al. [28] developed a machine learning approach that leverages historical trajectory and meteorological data to enhance the accuracy of aircraft trajectory prediction. Deep neural networks have become dominant tools across various domains, excelling in capturing complex relationships and efficiently handling large-scale datasets. Given the daily consistency of flight plans, Long Short-Term Memory (LSTM) [29] networks are particularly well-suited for capturing long-term dependencies and patterns in time series flight data. Shi et al. [21] introduced an LSTM-based trajectory prediction

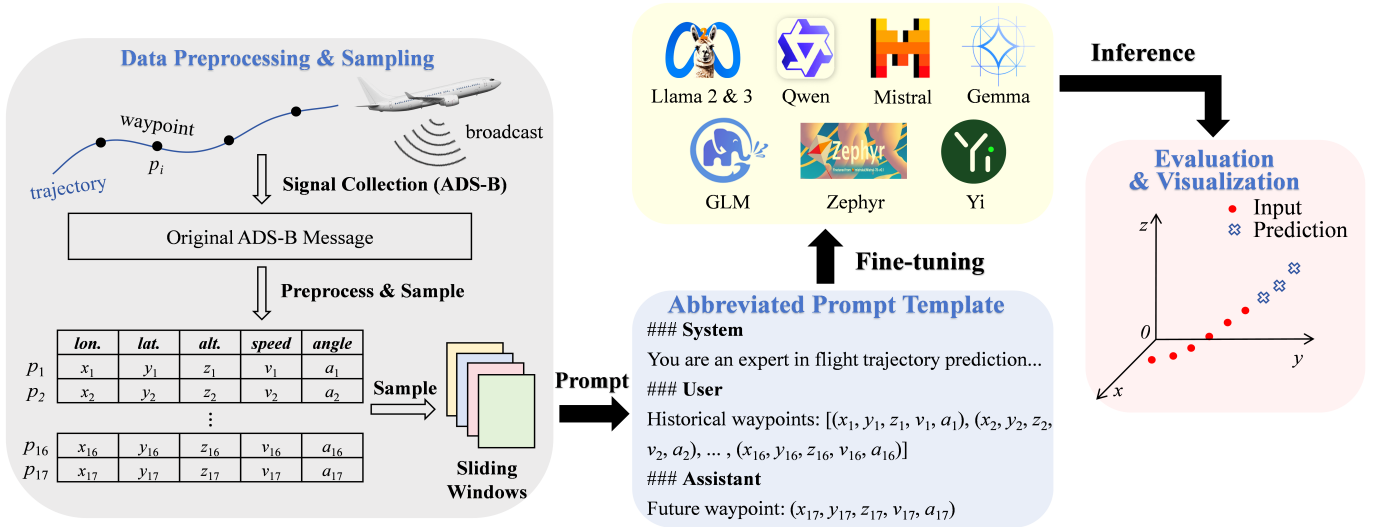


Fig. 3. Overall architecture of the proposed FTP-LLM, comprising data preprocessing, sliding window sampling, prompt construction, fine-tuning on LLMs, and inference for prediction.

model, achieving better accuracy compared to traditional models and establishing a robust foundation for anomaly detection and decision-making. Ma et al. [15] developed a hybrid CNN-LSTM model for aircraft trajectory prediction, where the CNN extracts spatial features from adjacent trajectory regions, and the LSTM captures temporal dependencies.

Originally proposed for machine translation, the Transformer [30] model has revolutionized deep learning through its innovative multi-head attention mechanism. Guo et al. [16] proposed FlightBERT, a Transformer-based framework for trajectory prediction, leveraging binary encoding and attribute correlation attention to capture complex motion patterns. Dong et al. [31] employed the Transformer network to develop a comprehensive trajectory prediction model that spans the entire flight phase, from takeoff to landing. Fan et al. [32] proposed a TCN-Informer model for aviation trajectory prediction, achieving high accuracy through spatiotemporal feature extraction and efficient temporal correlation.

B. Large Language Models

With the growing popularity and widespread application of Generative Pre-trained Transformers (GPT) [33], LLMs have emerged as leading tools for various domains. Extensive research has been carried out on time series tasks utilizing LLMs. Chang et al. [34] proposed LLM4TS, leveraging pre-trained LLMs for time-series forecasting through a two-stage fine-tuning process and PEFT techniques. Munir et al. [35] explored the feasibility of open-source LLMs for the ego-vehicle trajectory prediction problem in autonomous driving. Zhang et al. [36] applied the LLaMA model to flight trajectory reconstruction, demonstrating the efficiency of LLMs in handling noisy flight data but highlighting their limitations with long sequences due to token length constraints. Liu et al. [37] pioneered the use of LLMs for cuffless blood pressure estimation from wearable biosignals through context-enhanced prompts and instruction tuning.

III. METHODOLOGY

In this section, we present FTP-LLM, a framework for trajectory prediction, as illustrated in Fig. 3. We begin by explaining how LLMs can be applied to trajectory prediction, followed by a detailed description of the model architecture.

A. Problem Definition

Our objective is to predict an aircraft’s position over several successive time steps based on historical data. Specifically, the flight trajectory T is discretized into a sequence of waypoints:

$$T = \{T_{1:t}, T_{t+1:t+n}\}, \quad (1)$$

$$T_{1:t} = \{p_1, p_2, \dots, p_t\}, \quad (2)$$

$$T_{t+1:t+n} = \{p_{t+1}, p_{t+2}, \dots, p_{t+n}\}, \quad (3)$$

where a complete trajectory T is divided into two parts: $T_{1:t}$, representing the t previous waypoints, and $T_{t+1:t+n}$, denoting the n future waypoints. Each waypoint p_i captures the aircraft’s position and states at timestamp i , described by five attributes:

$$p_i = (x_i, y_i, z_i, v_i, a_i), \quad (4)$$

where x_i , y_i , z_i , v_i , and a_i correspond to longitude, latitude, altitude, speed, and heading angle, respectively.

LLMs are designed to process language inputs, while trajectory waypoints are numerical coordinates. To bridge this gap, we embed these coordinates into prompts and use an LLM tokenizer to convert the trajectory T into a sequence of language tokens:

$$T_{1:t} = \{p_1, p_2, \dots, p_t\} = \{w_1, w_2, \dots, w_n\}, \quad (5)$$

where w_j denotes the j -th token in a sentence. Typically, waypoint p_i is represented by a set of w_j . For instance, the longitude value “103.25” is split into three distinct tokens: “103”, “.”, and “25” using the LLaMA-3.1 tokenizer. In this

way, trajectory prediction can be viewed as a next token prediction process and treated as a language modeling problem:

$$\mathcal{L}_{\text{LLM}} = - \sum_{j=1}^N \log P(\hat{w}_j | w_1, w_2, \dots, w_{j-1}). \quad (6)$$

By performing data-to-tokens conversion on trajectory, we can then leverage LLMs to solve forecasting tasks. After decorating the trajectory with domain-specific prompt and fine-tuning LLMs on large-scale data, they can make trajectory predictions based on the learned probability distribution.

B. Model Architecture

1) *Data Preprocessing*: We collected flight trajectories of inbound and outbound, domestic and international flights at Guangzhou Baiyun International Airport (CAN), Beijing Capital International Airport (PEK), and Shanghai Pudong International Airport (PVG) to construct the datasets. A trajectory consists of multiple waypoints, each represented in ADS-B format and containing attributes such as timestamp, UTC time, callsign, longitude, latitude, altitude, velocity, and heading angle. Table I shows an example of ADS-B data. Incomplete, duplicate, and invalid trajectories (e.g., those with out-of-range latitude values) are first removed during preprocessing. Next, the values of longitude, latitude, altitude, velocity, and heading angle are rounded to 5, 5, 3, 3, and 2 decimal places, respectively. The raw ADS-B data, recorded at irregular intervals in seconds, are aggregated at the minute level to ensure temporal consistency. Specifically, for each interval, we realign the time unit by computing the average of longitude, latitude, altitude, velocity, and heading angle, respectively.

2) *Sliding Window Sampling*: A sliding window strategy is used to slice trajectories from the ADS-B data. To ensure continuity, the time interval within each window is strictly constrained to 1 minute, as aircraft may make stopovers during flight, leading to intermittent trajectory. Fig. 4 visualizes the sliding window strategy in detail. As shown in Fig. 4, the window size is set to 17 for single-step prediction, consisting of 16 consecutive time steps as input and 1 time step for prediction. For multi-step prediction, the window size is set to 20 or 24, corresponding to 4 or 8 prediction steps, respectively. The stride is set to be larger than the window size to prevent overlap and enhance data diversity.

3) *Prompt Design*: After processing and sampling the original ADS-B data, we populate the prompts with values of sliding windows. A typical chat-LLM prompt consists of

TABLE I
FEATURES OF ADS-B DATA

Feature	Unit	Waypoint
Timestamp	Unix	1727926166
UTC Time	/	2024-10-3 3:29:26
Call Sign	/	3S528
Longitude	Degree	13.61184
Latitude	Degree	50.48944
Altitude	Meter	10058.400
Velocity	Kilometer/Hour	968.596
Heading Angle	Degree	125.00

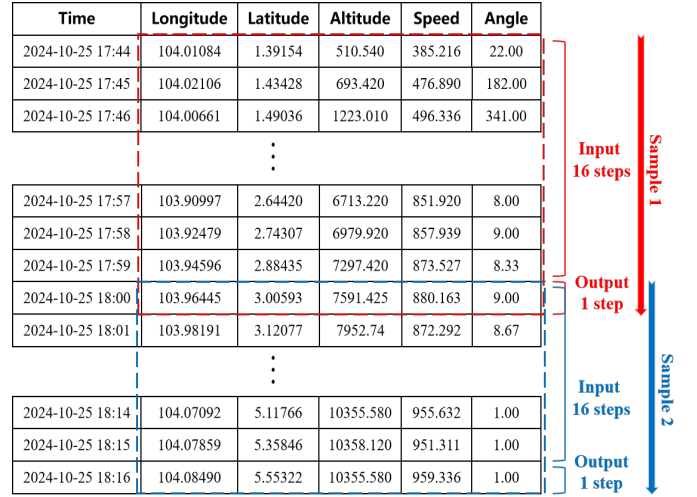


Fig. 4. Visualization of the sliding window strategy in single-step prediction.

```

SYSTEM
**Flight Trajectory Predictor**
Role: You are an expert in flight trajectory prediction. Predict future trajectory of an aircraft based on the historical flight data.
Input: Historical Trajectory
- Flight data of 16 waypoints, each represents a time step in the past and is formatted as a tuple (longitude, latitude, altitude, speed, heading angle).
- The time interval between each consecutive waypoint is within 1 minute.
- Positive longitude is east of the prime meridian, while negative longitude is west of the prime meridian.
- Positive latitude is north of the equator, while negative latitude is south of the equator.
Output: Future Trajectory
- Predict the aircraft's position in the next 4 time steps based on the past 16 waypoints.
- MOST IMPORTANT: Output the predicted position as 4 future waypoints, each in a tuple format (longitude, latitude, altitude, speed, heading angle).
- Only the coordinate is required. Do not include any additional information or reasoning behind the prediction.

USER
Flight data of the past 16 waypoints are as follows:\n [(112.08301, 24.55356, 7579.995, 859.328, 276.00), (111.93022, 24.56781, 8004.810, 854.698, 276.00), (111.81365, 24.57853, 8336.280, 843.277, 276.00), (111.69661, 24.58925, 8415.020, 832.165, 276.00), (111.54570, 24.60610, 8412.480, 834.326, 282.75), (111.43432, 24.66729, 8410.575, 813.491, 321.25), (111.36665, 24.77195, 8404.860, 807.009, 326.50), (111.27037, 24.85607, 8410.575, 813.954, 305.25), (111.16167, 24.92413, 8412.480, 814.880, 304.00), (111.05165, 24.99275, 8414.385, 815.343, 304.25), (110.93962, 25.06244, 8414.385, 815.343, 304.00), (110.83060, 25.13014, 8418.195, 814.695, 304.07), (110.71273, 25.20317, 8414.004, 812.695, 304.04), (110.60370, 25.27052, 8409.940, 812.781, 304.10), (110.49952, 25.33477, 8412.480, 812.797, 304.02), (110.38803, 25.40332, 8412.480, 810.296, 304.02)].

ASSISTANT
The predicted position in the next 4 time steps are as follows:\n [(110.27713, 25.47133, 8412.480, 808.398, 304.00), (110.16618, 25.53924, 8406.765, 809.787, 304.00), (110.05450, 25.60743, 8414.385, 810.713, 304.00), (109.94305, 25.67536, 8420.100, 810.157, 303.95)].

```

Fig. 5. An example of prompt template provided to LLMs.

three parts: system, user, and assistant. The system part elaborate the background and requirements of the flight trajectory prediction task, beginning with a role definition such as “You are an expert in flight prediction” to guide the model into the aviation domain. It also includes necessary terminology explanations and specifies output priorities. The user part provides waypoints from the previous 16 time steps in coordinate format to form a query. Finally, the assistant part contains the predicted waypoints for the next few time steps as the model’s response. During the fine-tuning phase, all three parts are incorporated into a single input using a specific tokenizer template. However, in the inference phase, the assistant part is masked, and the model generates predictions based only on the system and user parts. An example of prompts provided to LLMs is shown in Fig. 5.

IV. EXPERIMENTS

A. Experimental Configurations

We conducted experiments on eight state-of-the-art open-source LLMs with parameters around 7 billion from Hugging-

Face, including Gemma-2-9B [38], GLM-4-9B [39], LLaMA-2-7B [40], LLaMA-3.1-8B [41], Mistral-7B-v0.2 [42], Qwen-2.5-7B [43], Yi-1.5-9B [44], and Zephyr-7B-Beta [45]. For comparison, baseline trajectory prediction methods in this study include vanilla LSTM [21], BiLSTM [46] and Transformer [30]. To make a trade-off between model performance and computational efficiency, we adopted Low-Rank Adaptation (LORA) [47], a PEFT technique, combined with 4-bit quantization to reduce memory usage and computational overhead. The whole fine-tuning phase lasts for 3 epochs with the batch size set to 4 and the initial learning rate for Adam optimizer is set to 0.0002. Both fine-tuning and inference were executed on a single RTX 4090 GPU with 24 GB of memory.

B. Evaluation Metrics

Two commonly used metrics, Mean Absolute Error (MAE) and Root Mean Square Error (RMSE), are employed to evaluate the performance of models in flight trajectory prediction. MAE quantifies the average absolute error, indicating how closely the predicted values align with the ground truth. In contrast, RMSE measures the square root of the mean squared differences between the predicted values and the ground truth. Smaller MAE and RMSE values reflect higher accuracy in motion prediction. The mathematical definitions of MAE and RMSE are as follows:

$$\text{MAE} = \frac{1}{n} \sum_{i=1}^n |y - y'|, \quad (7)$$

$$\text{RMSE} = \sqrt{\frac{1}{n} \sum_{i=1}^n (y - y')^2}, \quad (8)$$

where y and y' denote the predicted and ground truth values of waypoint attributes, respectively. Additionally, average inference latency is introduced as a metric to evaluate the efficiency of a model. It is defined as the time delay between receiving a prompt and generating a prediction.

$$\text{Inference Latency} = \frac{1}{N} \sum_{i=1}^N t_i, \quad (9)$$

where N is the size of test dataset and t_i is the inference latency for i -th sample in the dataset.

C. Experimental Results

1) *Comparative Analysis*: The results of different models are presented in Table II. It is evident that LLMs outperform traditional deep learning methods in both single-step and multi-step prediction tasks. Among the LLMs, the Mistral-v0.2 model demonstrates the best performance in single-step prediction. For multi-step prediction, both LLaMA-3.1 and Zephyr-Beta models exhibit outstanding performance in the 4-step prediction task, with each achieving the best results in different metrics. However, in the 8-step prediction task, the LLaMA-3.1 surpasses all other models, achieving the lowest MAE and RMSE. For traditional deep learning models, the

Transformer outperforms LSTM and BiLSTM in both single-step and multi-step prediction tasks, primarily due to its multi-head self-attention mechanism, which helps to capture global relationships within the data. Furthermore, the performance of LSTM and BiLSTM is comparable, indicating that the bidirectional structure of BiLSTM does not provide significant advantages in this task, where future context is less critical. A general performance degradation is observed across all models as the prediction horizon increases, which can be attributed to the growing challenge of accurately predicting successive trajectory waypoints in a single prediction and the lack of external knowledge. In addition, prediction errors for altitude are significantly larger than those for longitude and latitude. On the one hand, this discrepancy arises because altitude changes frequently and drastically during flight, whereas longitude and latitude typically exhibit only minor variations. On the other hand, altitude values, ranging from thousands to tens of thousands, differ substantially in magnitude compared to longitude (-180° to 180°) and latitude (-90° to 90°).

While LLMs achieve competitive results in terms of MAE and RMSE, they suffer from high inference latency compared to traditional deep learning models. This is mainly due to their complex architectures as well as the massive number of parameters, which necessitate substantial computational resources. Among all LLMs, the LLaMA-3.1 model stands out for its relatively lower latency thanks to its distinctive tokenizer, which treats numerical values (e.g., “123”) as a single token rather than splitting them into individual tokens (e.g., “1”, “2”, “3”). Consequently, LLaMA-3.1 generates fewer tokens during inference and reduces the overall inference time.

2) *Flight Phase-based Analysis*: This study further evaluates the predictive performance of the LLaMA-3.1 model in different flight phases. Flight trajectory is usually divided into three primary phases: take-off, cruise, and landing. Obvious differences in prediction performance are observed in different phases, as shown in Table III.

Specifically, in terms of MAE and RMSE metrics for longitude and latitude, the landing phase achieves the highest accuracy, followed by the cruise phase, with the take-off phase exhibiting the largest errors. The reasons can be summarized as follows: the landing phase typically adheres to regulated descent paths, resulting in smoother trajectories. The cruise phase experiences occasional influences from air currents and route adjustments, causing slightly higher errors in longitude and latitude. The take-off phase involves rapid acceleration and steep climbs, making it the most challenging phase for accurate predictions.

However, when it comes to the MAE and RMSE metrics for altitude, the cruise phase demonstrates the best performance, while the landing and take-off phases exhibit relatively larger errors. This is because the aircraft operates more stably with minimal altitude fluctuations during cruise, enabling the model to better capture underlying patterns. In contrast, the dynamic and nonlinear altitude changes during the landing and take-off phases introduce irregularity, increasing the complexity of making predictions. These findings underscore the need

TABLE II
RESULTS OF DIFFERENT MODELS IN FLIGHT TRAJECTORY PREDICTION

Model	Prediction Steps	Inference Latency (s)	MAE ↓			RMSE ↓		
			longitude (°)	latitude (°)	altitude (m)	longitude (°)	latitude (°)	altitude (m)
Gemma-2-9B [38]	1	3.4534	0.0052	0.0044	22.3933	0.0097	0.0078	52.0669
	4	7.9925	0.0208	0.0173	78.2016	0.0448	0.0369	188.7158
	8	13.5666	0.0448	0.0413	143.2044	0.0981	0.0928	340.5264
GLM-4-9B [39]	1	1.6104	0.0056	0.0048	23.0343	0.0104	0.0087	52.7163
	4	4.5394	0.0185	0.0154	73.2479	0.0418	0.0358	181.1112
	8	8.2889	0.0472	0.0428	140.2281	0.1016	0.0941	341.4865
LLaMA-2-7B [40]	1	1.4704	0.0061	0.0051	23.7410	0.0114	0.0088	53.8996
	4	4.3878	0.0186	0.0150	72.4074	0.0419	0.0329	178.9544
	8	7.9162	0.0488	0.0445	147.4378	0.1039	0.0970	349.4891
LLaMA-3.1-8B [41]	1	1.0585	0.0053	0.0046	23.2201	0.0098	0.0081	53.4848
	4	4.2812	0.0169	0.0134	68.2341	0.0398	0.0304	174.7966
	8	6.6732	0.0434	0.0403	138.5888	0.0955	0.0904	336.9702
Mistral-7B-v0.2 [42]	1	2.1465	0.0051	0.0042	21.2091	0.0097	0.0077	49.9429
	4	6.3397	0.0171	0.0142	70.9545	0.0398	0.0328	178.0764
	8	9.4770	0.0457	0.0430	147.3300	0.1005	0.0975	347.3605
Qwen-2.5-7B [43]	1	1.8655	0.0055	0.0050	23.3936	0.0102	0.0171	53.6241
	4	5.3395	0.0186	0.0152	73.4411	0.0427	0.0335	178.6826
	8	10.2877	0.0477	0.0445	148.1366	0.1012	0.0986	344.7497
Yi-1.5-9B [44]	1	2.1667	0.0055	0.0053	23.6459	0.0107	0.0190	53.3111
	4	7.9780	0.0181	0.0149	71.3618	0.0417	0.0330	177.8078
	8	12.4595	0.0465	0.0439	147.4845	0.1015	0.0985	350.9740
Zephyr-7B-Beta [45]	1	2.1434	0.0059	0.0054	24.1520	0.0113	0.0124	54.7890
	4	6.7279	0.0166	0.0137	68.4934	0.0391	0.0314	173.6565
	8	9.2350	0.0469	0.0441	153.6472	0.1017	0.0983	360.0954
LSTM [21]	1	0.0006	0.0065	0.0060	27.1511	0.0116	0.0100	59.2235
	4	0.0006	0.0201	0.0167	82.2635	0.0436	0.0368	185.5921
	8	0.0008	0.0488	0.0460	158.6258	0.1038	0.0994	368.4862
BiLSTM [46]	1	0.0006	0.0066	0.0062	27.6808	0.0119	0.0105	60.3736
	4	0.0007	0.0203	0.0169	83.1023	0.0441	0.0370	187.6258
	8	0.0009	0.0491	0.0457	160.1134	0.1045	0.1002	372.4689
Transformer [30]	1	0.0007	0.0059	0.0055	26.0105	0.0108	0.0098	57.8672
	4	0.0009	0.0190	0.0161	80.1597	0.0417	0.0351	184.3560
	8	0.0010	0.0484	0.0447	156.2346	0.1017	0.0987	357.4765

TABLE III
RESULTS OF THE LLaMA-3.1 MODEL IN DIFFERENT FLIGHT PHASES

Model	Prediction Steps	Phase	MAE ↓			RMSE ↓		
			longitude (°)	latitude (°)	altitude (m)	longitude (°)	latitude (°)	altitude (m)
LLaMA-3.1-8B [41]	1	Entire	0.0053	0.0046	23.2201	0.0098	0.0081	53.4848
		Take-off	0.0052	0.0045	57.5784	0.0092	0.0078	87.0801
		Cruise	0.0058	0.0047	16.7268	0.0103	0.0082	47.1502
		Landing	0.0029	0.0042	26.7520	0.0066	0.0078	44.7281
	4	Entire	0.0169	0.0134	68.2341	0.0398	0.0304	174.7966
		Take-off	0.0196	0.0161	169.8109	0.0415	0.0328	282.7475
		Cruise	0.0179	0.0137	52.3356	0.0416	0.0315	160.0391
		Landing	0.0106	0.0098	70.6739	0.0282	0.0221	136.0483
	8	Entire	0.0434	0.0403	138.5888	0.0955	0.0904	336.9702
		Take-off	0.0553	0.0638	351.9017	0.1104	0.1218	571.8308
		Cruise	0.0500	0.0439	86.0120	0.1084	0.0956	275.0546
		Landing	0.0389	0.0337	149.5462	0.0881	0.0794	254.8113

for models that incorporate the unique characteristics of each flight phase and encourage further research on phase-specific algorithms to enhance accuracy.

3) *Visualization Analysis*: To provide an intuitive comparison, we visualize the prediction results of different models

in 8-step predictions. Fig. 6 depicts representative scenarios in different flight phases. In Fig. 6(a), all models demonstrate accurate predictions, as the flight maintains a constant cruise altitude during this phase. In Fig. 6(b) and Fig. 6(c), all models successfully capture the overall trajectory trends, with slight

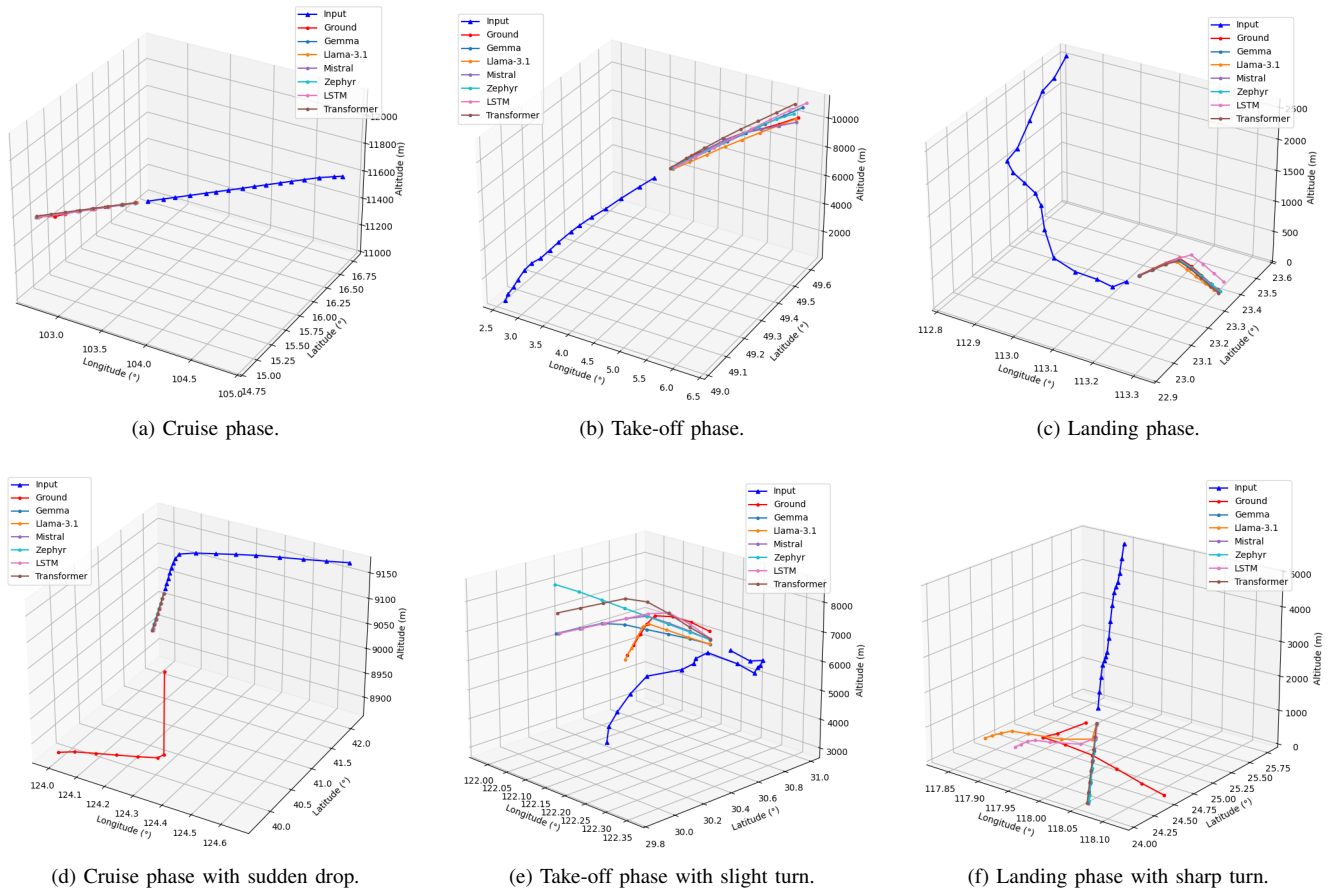


Fig. 6. Visualization of 8-step prediction results in different flight phases. Blue for input, red for ground truth.

discrepancies observed between the predictions and the ground truth. The last three figures illustrate special cases encountered during flight. In Fig. 6(d), the flight initially maintains a stable altitude; however, an abrupt altitude drop of approximately 200 meters occurs at the first step of the prediction horizon, causing all models to fail in producing accurate predictions. Fig. 6(e) presents a slight turning maneuver in the future trajectory, which is effectively captured by the LLaMA-3.1 model, while other models exhibit poorer performance. Finally, in Fig. 6(f), most models incorrectly predict that the aircraft will continue descending without turning. Unlike those models, the LLaMA-3.1 and Transformer models show some ability to recognize signs of a potential turn. However, they still can't make satisfactory predictions in the end.

It can be observed from these figures that the predictive performance during the cruise phase is better than that during the take-off and landing phases. This is mainly due to the aircraft's stability during the cruise phase, which allows for more accurate trajectory predictions. However, unanticipated maneuvers during flight increase complexity that far exceeds the capabilities of fine-tuned LLMs, underscoring the need for further research.

4) *Few-shot Learning*: Furthermore, we investigated the generalization capability of LLMs, an essential aspect that distinguishes them from traditional deep learning methods.

We conducted 4-step prediction experiments solely on the LLaMA-3.1 model, splitting the training data into different proportions: 1%, 5%, 10%, 30%, and 50%. As presented in Table IV, the results show that the LLaMA-3.1 model can still achieve satisfactory performance even with a limited amount of training data (approximately 30%). This highlights its extensive pre-trained knowledge and powerful generalization as well as transfer learning abilities in few-shot learning scenarios. More importantly, these experiments offer the insight that, in contrast to traditional deep learning-based models which typically demand tremendous training data, LLaMA-3.1 is particularly well-suited for data-limited situations.

5) *Failure Analysis*: We observed a number of failure cases when using the Yi-1.5 model during inference, as illustrated in Fig. 7. In Fig. 7(a), the future trajectory is missing entirely. In Fig. 7(b), the output contains a complete trajectory, but is presented in an incorrect format, failing to represent it as coordinates. In Fig. 7(c), the prediction deviates significantly from the ground truth. The longitude value at the next time step is expected to be positive, yet the Yi-1.5 model outputs a negative value instead. This issue may result from insufficient fine-tuning of the model to comprehend the implications of a negative sign in longitude or latitude. To ensure the reliability of metrics, cases with severe deviations are excluded when calculating MAE and RMSE.

TABLE IV
FEW-SHOT LEARNING PERFORMANCE BETWEEN LLAMA-3.1 AND DEEP LEARNING MODELS

Model	Proportion	MAE ↓			RMSE ↓		
		longitude (°)	latitude (°)	altitude (m)	longitude (°)	latitude (°)	altitude (m)
LLaMA-3.1-8B [41]	1 %	0.0251	0.0214	98.8880	0.0500	0.0439	216.2459
	5 %	0.0230	0.0192	89.7103	0.0476	0.0387	201.7122
	10 %	0.0216	0.0176	84.1962	0.0471	0.0364	193.5335
	30 %	0.0200	0.0166	81.5059	0.0440	0.0349	192.2510
	50 %	0.0189	0.0155	77.2418	0.0423	0.0340	186.8130
	100 %	0.0169	0.0134	68.2341	0.0398	0.0304	174.7966
LSTM [21]	100 %	0.0201	0.0167	82.2635	0.0436	0.0368	185.5921
BiLSTM [46]	100 %	0.0203	0.0169	83.1023	0.0441	0.0370	187.6258
Transformer [30]	100 %	0.0190	0.0161	80.1597	0.0417	0.0351	184.3560

Based on the historical flight data provided, the predicted position of the aircraft in the next time step is:

(a) Missing trajectory.

The aircraft's position in the next time step is predicted to be at a longitude of 107.68495, latitude of 32.12254, altitude of 11612.880.

(b) Unexpected format.

Prediction

The predicted position in the next time step is (-111.3768, 37.3590, 9784.08).

Ground

The predicted position in the next time step is (111.27851, 37.3577, 9784.08).

(c) Severe deviation.

Fig. 7. Failure cases in the Yi-1.5 model.

V. CONCLUSION AND FUTURE WORK

In this paper, we pioneer the use of LLMs in flight trajectory prediction. Through comprehensive experiments on real ADS-B data, we demonstrated the potential of LLMs for both single-step and multi-step predictions compared to traditional deep learning-based methods. Besides, the visualization results showed that they can effectively understand and capture the underlying trajectory patterns across different phases. Moreover, generalization experiments on the LLaMA-3.1 model revealed that LLMs can make satisfactory predictions even with limited training data, highlighting their extensive pre-trained knowledge and strong transfer learning capability.

Even though LLMs exhibit strength in predicting future trajectory, their severe and unacceptable inference latency, especially as the prediction horizon extends, prevents them from meeting the requirements of real-time air traffic systems. To address this problem, inference acceleration techniques must be considered in future work. Regarding challenges, on the one hand, LLMs yield less accurate results when unexpected operations occur during flight, such as sudden drops or sharp turns. On the other hand, prediction errors vary significantly across different flight phases, emphasizing the need for advanced algorithms tailored to each phase. Future research should focus on improving the robustness and accuracy of LLMs in flight trajectory prediction.

ACKNOWLEDGMENT

This work is supported in part by the National Natural Science Foundation of China (NSFC 62371325).

REFERENCES

- [1] Z. Zhang, D. Guo, S. Zhou, J. Zhang, and Y. Lin, "Flight trajectory prediction enabled by time-frequency wavelet transform," *Nat. Commun.*, vol. 14, no. 1, p. 5258, Aug. 2023.
- [2] M. Strohmeier, M. Schäfer, V. Lenders, and I. Martinovic, "Realities and challenges of nextgen air traffic management: The case of ads-b," *IEEE Commun. Mag.*, vol. 52, no. 5, pp. 111–118, May 2014.
- [3] T. Bolić and P. Ravenhill, "Sesar: The past, present, and future of european air traffic management research," *Engineering*, vol. 7, no. 4, pp. 448–451, 2021.
- [4] K. Cate, "Challenges in achieving trajectory-based operations," in *51st AIAA Aerospace Sciences Meeting Including the New Horizons Forum and Aerospace Exposition*, Jan. 2013, p. 443.
- [5] Z. Chen, D. Guo, and Y. Lin, "A deep gaussian process-based flight trajectory prediction approach and its application on conflict detection," *Algorithms*, vol. 13, no. 11, p. Art. no. 11, Nov. 2020.
- [6] M. Mamdouh, M. Ezzat, and H. Hefny, "Improving flight delays prediction by developing attention-based bidirectional lstm network," *Expert Syst. Appl.*, vol. 238, p. 121747, 2024.
- [7] Y. Zhang *et al.*, "Short-term multi-step-ahead sector-based traffic flow prediction based on the attention-enhanced graph convolutional lstm network (agc-lstm)," *Neural Computing and Applications*, pp. 1–20, 2024.
- [8] D. Guo, Z. Zhang, Z. Yan, J. Zhang, and Y. Lin, "Flightbert++: A non-autoregressive multi-horizon flight trajectory prediction framework," in *Proc. AAAI Conf. Artif. Intell.*, vol. 38, 2024, pp. 127–134.
- [9] Z. Wang, M. Liang, and D. Delahaye, "Short-term 4d trajectory prediction using machine learning methods," in *SID 2017, 7th SESAR Innovation Days*, 2017.
- [10] T. Wang, "4d flight trajectory prediction model based on improved kalman filter," *Journal of Computer Applications*, vol. 34, no. 6, p. 1812, 2014.
- [11] R. Rezaie and X. R. Li, "Trajectory modeling and prediction with waypoint information using a conditionally markov sequence," in *Proc. 2018 56th Annu. Allerton Conf. Commun., Control, Comput. (Allerton)*, Oct. 2018, pp. 486–493.
- [12] W. Schuster, "Trajectory prediction for future air traffic management—complex manoeuvres and taxiing," *The Aeronautical Journal*, vol. 119, no. 1212, pp. 121–143, 2015.
- [13] W. Zeng, Z. Quan, Z. Zhao, C. Xie, and X. Lu, "A deep learning approach for aircraft trajectory prediction in terminal airspace," *IEEE Access*, vol. 8, pp. 151 250–151 266, 2020.
- [14] Y. Fan, Y. Tan, L. Wu, H. Ye, and Z. Lyu, "Global and local inter-attribute relationships based graph convolutional network for flight trajectory prediction," *IEEE Transactions on Aerospace and Electronic Systems*, 2024.
- [15] L. Ma and S. Tian, "A hybrid cnn-lstm model for aircraft 4d trajectory prediction," *IEEE Access*, vol. PP, no. 99, pp. 1–1, 2020.

- [16] D. Guo *et al.*, “Flightbert: Binary encoding representation for flight trajectory prediction,” *IEEE Trans. Intell. Transp. Syst.*, vol. 24, no. 2, pp. 1828–1842, Feb. 2023.
- [17] D. Zhu, J. Chen, X. Shen, X. Li, and M. Elhoseiny, “Minigt-4: Enhancing vision-language understanding with advanced large language models,” *arXiv preprint arXiv:2304.10592*, 2023.
- [18] S. Li, B. Li, B. Sun, and Y. Weng, “Towards visual-prompt temporal answer grounding in instructional video,” *IEEE Transactions on Pattern Analysis and Machine Intelligence*, 2024.
- [19] Y. Fathullah *et al.*, “Prompting large language models with speech recognition abilities,” in *Proc. ICASSP 2024 - IEEE Int. Conf. Acoust., Speech Signal Process. (ICASSP)*, 2024, pp. 13 351–13 355.
- [20] J. Mao, Y. Qian, J. Ye, H. Zhao, and Y. Wang, “Gpt-driver: Learning to drive with gpt,” *arXiv preprint arXiv:2310.01415*, 2023.
- [21] Z. Shi, M. Xu, Q. Pan, B. Yan, and H. Zhang, “Lstm-based flight trajectory prediction,” in *Proc. 2018 Int. Joint Conf. Neural Netw. (IJCNN)*, 2018, pp. 1–8.
- [22] D. Chao *et al.*, “Three-dimension collision-free trajectory planning of uavs based on ads-b information in low-altitude urban airspace,” *Chinese Journal of Aeronautics*, vol. 38, no. 2, p. 103170, 2025.
- [23] H. Jeung, H. T. Shen, and X. Zhou, “Mining trajectory patterns using hidden markov models,” in *Proc. Int. Conf. Data Warehousing and Knowledge Discovery*, 2007, pp. 470–480.
- [24] W. Zeng, X. Chu, Z. Xu, Y. Liu, and Z. Quan, “Aircraft 4d trajectory prediction in civil aviation: A review,” *Aerospace*, vol. 9, no. 2, p. Art. no. 2, Feb. 2022.
- [25] J. Sun, J. Ellerbroek, and J. Hoekstra, “Modeling and inferring aircraft takeoff mass from runway ads-b data,” in *7th International Conference on Research in Air Transportation*, 2016.
- [26] J. A. Besada, G. Frontera, J. Crespo, E. Casado, and J. López-Leonés, “Automated aircraft trajectory prediction based on formal intent-related language processing,” *IEEE Trans. Intell. Transp. Syst.*, vol. 14, no. 3, pp. 1067–1082, Sep. 2013.
- [27] K. Tastambekov, S. Puechmorel, D. Delahaye, and C. Rabut, “Aircraft trajectory forecasting using local functional regression in sobolev space,” *Transp. Res. Part C: Emerg. Technol.*, vol. 39, pp. 1–22, 2014.
- [28] A. D. Leege, M. van Paassen, and M. Mulder, “A machine learning approach to trajectory prediction,” in *Proc. AIAA Guidance, Navigation, and Control (GNC) Conf.*, 2013, p. 4782.
- [29] S. Hochreiter, “Long short-term memory,” *Neural Computation MIT-Press*, 1997.
- [30] A. Vaswani *et al.*, “Attention is all you need,” in *Advances in Neural Information Processing Systems (NeurIPS)*, 2017, pp. 5998–6008.
- [31] X. Dong, Y. Tian, K. Niu, M. Sun, and J. Li, “Research on flight trajectory prediction method based on transformer,” in *Proc. Int. Conf. Smart Transp. City Eng. (STCE 2023)*, M. Mikusova, Ed. Chongqing, China: SPIE, 2024, p. 235.
- [32] Z. Dong *et al.*, “Tcn-informer-based flight trajectory prediction for aircraft in the approach phase,” *Sustainability*, vol. 15, no. 23, p. 16344, 2023.
- [33] A. Radford, K. Narasimhan, T. Salimans, and I. Sutskever, “Improving language understanding by generative pre-training,” 2018.
- [34] C. Chang, W.-C. Peng, and T.-F. Chen, “Llm4ts: Two-stage fine-tuning for time-series forecasting with pre-trained llms,” *arXiv preprint arXiv:2308.08469*, 2023.
- [35] F. Munir, T. Mihaylova, S. Azam, T. P. Kucner, and V. Kyrki, “Exploring large language models for trajectory prediction: A technical perspective,” in *Companion of the 2024 ACM/IEEE Int. Conf. Human-Robot Interaction*. Boulder, CO, USA: ACM, 2024, pp. 774–778.
- [36] Q. Zhang and J. H. Mott, “An exploratory assessment of llm’s potential toward flight trajectory reconstruction analysis,” *arXiv preprint arXiv:2401.06204*, 2024.
- [37] Z. Liu *et al.*, “Large language models for cuffless blood pressure measurement from wearable biosignals,” in *Proc. 15th ACM Int. Conf. Bioinformatics, Computational Biology and Health Informatics (BCB ’24)*. Shenzhen, China: ACM, 2024, pp. 1–11.
- [38] G. Team *et al.*, “Gemma 2: Improving open language models at a practical size,” *arXiv preprint arXiv:2408.00118*, 2024.
- [39] T. GLM *et al.*, “Chatglm: A family of large language models from glm-130b to glm-4 all tools,” *arXiv preprint arXiv:2406.12793*, 2024.
- [40] H. Touvron *et al.*, “Llama 2: Open foundation and fine-tuned chat models,” *arXiv preprint arXiv:2307.09288*, 2023.
- [41] A. Grattafiori *et al.*, “The llama 3 herd of models,” *arXiv preprint arXiv:2407.21783*, 2024.
- [42] A. Q. Jiang *et al.*, “Mistral 7b,” *arXiv preprint arXiv:2310.06825*, 2023.
- [43] A. Yang *et al.*, “Qwen2.5 technical report,” *arXiv preprint arXiv:2412.15115*, 2025.
- [44] A. Young *et al.*, “Yi: Open foundation models by 01.ai,” *arXiv preprint arXiv:2403.04652*, 2024.
- [45] L. Tunstall *et al.*, “Zephyr: Direct distillation of lm alignment,” *arXiv preprint arXiv:2310.16944*, 2023.
- [46] M. Schuster and K. K. Paliwal, “Bidirectional recurrent neural networks,” *IEEE Trans. Signal Process.*, vol. 45, no. 11, pp. 2673–2681, 1997.
- [47] E. J. Hu *et al.*, “Lora: Low-rank adaptation of large language models,” in *Proc. Int. Conf. Learn. Representations (ICLR)*, 2022.